Development 126, 483-494 (1999)
Printed in Great Britain © The Company of Biologists Limited 1999
DEV3933

Abrogation of the *Cripto* gene in mouse leads to failure of postgastrulation morphogenesis and lack of differentiation of cardiomyocytes

Chunhui Xu[1], Giovanna Liguori[2], M. Graziella Persico[2] and Eileen D. Adamson[1,*]

[1]The Burnham Institute, La Jolla Cancer Research Center, 10901, N. Torrey Pines Road, La Jolla, CA 92037, USA
[2]Instituto Internationale di Genetica e Biofisica, Via Gugliemi Marconi, Napoli, Italy
*Author for correspondence (e-mail: eadamson@burnham-inst.org)

Accepted 10 November 1998; published on WWW 7 January 1999

SUMMARY

Cripto-1(Cr1) protein encoded by the *tdgf1* gene, is a secreted growth factor that is expressed early in embryonic development and is re-expressed in some tumors of the breast and colon. During embryonic development, Cr1 is expressed in inner cell mass cells and the primitive streak, and later is restricted to the developing heart. To investigate the role of Cr1 during mouse development, mice were generated that contain a null mutation of both *Cr1* genes, derived from homologous recombination in embryonic stem cells. No homozygous $Cr1^{-/-}$ mice were born, indicating that Cr1 is necessary for embryonic development. Embryos initiated gastrulation and some embryos produced mesoderm up to day E7.5. Increasingly aberrant morphogenesis gave rise to disordered neuroepithelium that failed to produce a recognizable neural tube, or head-fold. Although some biochemical markers of differentiating ectoderm, mesoderm and endoderm were expressed, all the cardiac-specific markers were absent from day E8.7 embryos: αMHC, βMHC, MLC2A, MLC2V and ANF, whereas they were expressed in wild-type embryos. The yolk sac and placental tissues continued development in the absence of the embryo until day E9.5 but lacked large yolk sac blood vessels. Chimeric mice were constructed by microinjection of double targeted $Cr1^{-/-}$ embryonic stem cells into normal C57BL/6 blastocysts. The Cr1 produced by the normal C57BL/6 cells fully rescued the phenotype of $Cr1^{-/-}$ cells, indicating that Cr1 protein acted in a paracrine manner. Cells derived from the embryo proliferated and migrated poorly and had different adhesion properties compared to wild type. Therefore, lethality in the absence of Cr1, likely resulted largely from defective precardiac mesoderm that was unable to differentiate into functional cardiomyocytes.

Key words: Gene targeting, Homologous recombination, Mesoderm, Visceral endoderm, Neuroepithelium, Gastrulation, Cardiac myosin, Mouse

INTRODUCTION

The mouse *Cripto-1 (Cr1)* gene, also known as teratocarcinoma-derived growth factor1 (*tdgf1*), encodes a growth factor, Cr1 (a 24-26 kDa glycoprotein) containing a modified Epidermal Growth Factor (EGF)-like domain (Ciccodicola et al., 1989). In Cr1, two of the three bicysteine loops in the EGF-domain are truncated, and it fails to bind to the EGF receptor (Brandt et al., 1994) or other type I receptor tyrosine kinases in the ErbB family (Kannan et al., 1997). Rather, Cr1 is a member of a different family (Shen et al., 1997) and interacts with an as yet unidentified receptor and activates intracellular components through ras/raf/MAPK pathway (Kannan et al., 1997). The mouse Cr1, like the human homologue CR1 (Dono et al., 1991) is encoded by 6 exons with exon 4 containing the EGF-like domain (Liguori et al., 1996). In addition, there are two *Cr1*-related pseudogenes, *Cr2* and *Cr3*, in the mouse genome; both of them lack introns and *Cr3* has many stop codons within the region corresponding to the Cr1 coding sequence (Liguori et al., 1996). Of these genes, only *Cr1* is expressed in teratocarcinoma F9 cells (our unpublished data) and embryo stem (ES) cells.

Cr1 has been implicated as playing roles during development. The earliest expression of Cr1 is in both trophoblast and inner cell mass cells of 4-day mouse blastocysts (Johnson et al., 1994). At day 6.5, the primitive streak stage, Cr1 is present in epiblast cells, ectoplacental cone and forming mesoderm, but later is restricted to the developing heart (Dono et al., 1993; Johnson et al., 1994). Cr1 is specifically expressed in the myocardium of the developing heart tubes in 8.5-day-old embryos and in the outflow region, conotruncus, of the heart at 9.5-10 days of gestation, when the heart develops into a functional chambered organ (Johnson et al., 1994). After 10.5 days of development, no in situ hybridization signals have been detected. Such a restricted pattern of Cr1 expression suggests a role in the important process of gastrulation, wherein the ectoderm germ layer gives

rise to the mesoderm tissues, including those producing the heart.

The highly restricted expression patterns of Cr1 in the developing embryo raise the possibility that Cr1 may play roles in cardiac morphogenesis. In support of this, we have recently shown that disruption of both Cr1 alleles by homologous recombination in ES cells leads to a specific block in the differentiation in vitro, of cardiac myocytes, which again suggests that this growth factor plays a role in the specification of cardiac tissues (Xu et al., 1998). To determine the function(s) of the Cr1 during development, we have generated *Cr1* null mice and found that inactivation of Cr1 leads to embryonic abnormalities around day E7.5. The anteroposterior axis fails to form and the primitive heart tube is not initiated. Our results show that the embryonic lethality in *Cr1* null mice might be a consequence of reduced and/or defective mesoderm failing to generate the precardiac mesodermal field from which the heart usually develops.

MATERIALS AND METHODS

Generation of chimeric mice carrying the disrupted Cr1 allele

Embryonic stem (R1 ES) cells were maintained in the undifferentiated state by standard protocols (Robertson, 1987). Two targeted ES $Cr1^{+/-}$ clones were prepared as described previously (Xu et al., 1998) were expanded and used to generate chimeric mice. To obtain chimeras, 10-15 ES cells were microinjected into blastocysts isolated at 3.5 days postcoitum from C57BL/6 pregnant female mice and then implanted into the uteri of CD-1 pseudopregnant recipient mice (Bradley, 1987). The male chimeras, identified by agouti coat color, were bred with Black Swiss female animals to test for germline transmission. Offspring with agouti coat color were tested for the presence of the targeted allele by PCR analysis. Animals that tested positive for the targeted allele were heterozygous and these were bred with heterozygous littermates to generate homozygotes. To analyze the mutation in an inbred genetic background, the chimeras were bred with 129 SvJ females and germline transmission of the targeted allele was screened by PCR analysis. Similarly, heterozygous males were bred into the C57BL/6 genetic background to analyze for differences in the phenotype. For the generation of chimeric animals consisting of $Cr1^{-/-}$ ES cells and wild-type $Cr1^{+/+}$ cell, two clones of $Cr1^{-/-}$ ES cells were karyotyped and one, DE14, appeared normal (Xu et al., 1998). DE14 cells were injected into 80-100 C57BL/6 blastocysts and the embryos were transplanted into pseudopregnant foster mothers. Tissues from either E14.5 individual embryos or from 10-day-old mice were dissected and homogenized for assay to determine their distribution of glucose phosphate isomerase (GPI) isoenzymes as described (Bradley, 1987). The $Cr1^{-/-}$ contribution was determined by comparison of the intensity of GPI-1a from the 129SvJ ES cells and the GPI-1b from the C57BL/6 blastocyst, analyzed by the NIH image software.

Genotyping of adults and embryos

Genotypes of mice were determined by PCR analysis of genomic DNA from tail biopsies. For embryos, yolk sac or whole embryos were used. Tail, yolk sac or embryos were resuspended in lysis buffer (50 mM Tris-HCl, pH 8.0, 20 mM NaCl, 0.1% SDS and 1 mg/ml proteinase K) and sequentially incubated at 55°C for 2-16 hours and 94°C for 10 minutes. The lysates were then subjected to PCR analysis. Sections of embryos were genotyped by scraping embryo tissue from several sections on slides, and pooling them into 30 μl lysis buffer. The lysates contained 1× PCR buffer and 60 μg/ml proteinase K, and were overlaid with mineral oil for incubation at 55°C for 2 hours and 95°C for 10 minutes. 10 μl of the lysate was transferred into tubes for each PCR reaction. The following primers were used for the PCR analysis: a set of primers within intron 3, 5′-GTCCCTGATAGTCTCTGATATTC-3′ (p-5) and 5′-GAAATGTAAGAAAAGTCATGGGG-3′ (p-6), to detect the wild-type allele. For detecting the targeted allele, a set of primers in the *neo* gene, 5′-GTCAAGAAGGCGATAGAAGGCGATGCG-3′ (p-7) and 5′-GGTGGAGAGGCTATTCGGCTATGACTG-3′ (p-8), or the primer set of p-1 and p-3 used in screening of ES cells was used (Xu et al., 1998). The reaction for primer p-5/p-6 and p-7/p-8 was performed by denaturing the DNA at 94°C for 2 minutes, followed by 35 cycles of amplification: 94°C for 30 seconds, 55°C for 30 seconds, 72°C for 1.5 minutes and a final extension step at 72°C for 6 minutes. For embryos in paraffin sections, 50 cycles were applied.

Blastocyst and embryo outgrowth

Embryos were designated as 0.5 days post coitum (p.c.) at noon on the morning of finding the copulation plug. Embryos designated as E7.7 or E8.7 were examined during the afternoon of the appropriate day of gestation. However, a developmental range occurs even within one litter. Blastocysts (E3.5) were collected in M2 medium (Hogan et al., 1993) and then transferred to medium containing high-glucose DMEM, 20% fetal bovine serum, 0.1 mM β-mercaptoethanol, 1 mM sodium pyruvate, 1× non-essential amino acid, 2 mM glutamine, 100 units of penicillin per ml and 0.1 mg of streptomycin (ES medium lacking LIF) in 24-well plates coated with gelatin. The cultures were examined for attachment and growth, photographed and collected for genotyping.

Embryo cultures for differentiation tests

Embryos (stage E7.7 when the mutant embryos were detectable by altered morphology) were dissected from decidual tissue. The egg cyclinders were isolated from the trophectoderm, ectoplacental cone and parietal endoderm, cut open with needles and transferred to the ES medium (described above) containing 20% FCS in 48-well plates. The cultures were allowed to proliferate for 2 weeks, examined for differentiated tissues and beating cardiomyocytes, and collected for genotyping. Similarly, E8.5 embryos were cultured in ES medium containing 10% FBS for 2 days and examined for beating cardiomyocytes. The cultures were then treated with collagenase IV (1 mg/ml, Atlanta Biologicals, Norcross, GA) for 1 hour at 37°C to partially dissociate the cells, seeded into wells to proliferate for 3-4 days and examined for neuron growth. Cells were collected for genotyping.

Embryo-derived fibroblast (MEF) cultures

Embryos (E8.5) from heterozygous breeding were dissected from decidual tissue and isolated from the trophectoderm, ectoplacental cone and parietal endoderm, dissociated with needles in medium containg high-glucose DMEM, 10% FCS, 1× non-essential amino acids (Sigma Chemical Corp. St Louis, MI), 1 mM sodium pyruvate and 0.1 mM β-mercaptoethanol and cultured in individual wells in a 48-well tissue-culture plate. Cells were trypsinized and transferred to 24-well plates after 2 days and passaged into 6-well plates after another 2 days. Mouse embryo fibroblasts (MEFs) were used for assays before passage 10. For genotype analysis, small pellets of cells were incubated in 30 μl lysis buffer containing 1× PCR buffer and 60 μg/ml proteinase K, overlaid with oil, at 55°C overnight and then 94°C for 12 minutes. 10 μl of the lysate was used for PCR reaction using primers 5, 6, 7 and 8 described above.

Cell proliferation assays (MTT, Promega, Madison WI)

MTT assays measure the ability of cells to metabolize 3-(4,5-dimethyldiazol-2-yl)-2,5-diphenyl tetrazolium bromide (MTT) to detect the numbers of cells after a period of proliferation. MEFs of all genotypes were dissociated and seeded into 96-well tissue-culture

plates at a density of 8×10^3 cells per well in 100 μl medium. At different time points, 15 μl of MTT solution was added to each well and incubated for 4 hours. The colored products were solubilized in 100 μl of solubilization solution, and a microtiter plate reader was used to measure absorbance at 590/650 nm. Results were expressed as mean ± standard deviation of values from three wells for each cell line. Similar results were obtained for three different embryos of each genotype.

Attachment assays

96-well plates (Linbro/Titertek, Flow Lab. Inc, McLean, VA) were incubated with 20 μg/ml of fibronectin, collagen I, collagen IV or laminin (Becton-Dickinson, Franklin Lakes, NJ) diluted in PBS at 4°C overnight. The wells were rinsed 3 times with PBS and blocked with 100 μl of 2% heat-denatured BSA at room temperature for 2 hours and rinsed 3 times with PBS. Cells were harvested in trypsin-EDTA and 100 μl (5×10^5 cells/ml) was added to each well in serum-free DMEM medium and allowed to attach for 40 minutes. Non-adherent cells were removed by gently washing 3 times with PBS and attached cells were fixed in 10% formalin at room temperature for 30 minutes and then stained with 1% toluidine blue for 60 minutes. The plates were washed extensively with water and air dried. The blue dye was eluted in 100 μl of 2% SDS solution and the absorbance was measured at OD_{620} on microtiter plate reader. Nonspecific cell adhesion was measured on BSA-coated wells and was subtracted from each reaction value.

Cell motility assays

(1) Haptotactic assays

Cell migration assays were performed essentially as described (Mansfield and Suchard, 1994), by using modified Boyden chambers (24-well cell culture insert, 8.0 μm pore size, Becton Dickinson, Franklin Lakes, NJ). To measure migration toward different matrix proteins, the lower surface of the membrane was coated with 20 μg/ml collagens Type I, Type IV, laminin or fibronectin overnight at 4°C. Cells were harvested with trypsin/EDTA, resuspended to 2.5×10^5 cells /ml and added to the upper chamber in 500 μl medium. The lower chamber was filled with 1 ml medium. After 24 hours incubation at 37°C, the upper surface of the membrane was wiped with a cotton tip to remove the nonmigated cells. The cells that had migrated through the pores to the underside of the membrane were fixed with 4% formaldehyde and stained with crystal violet. The numbers of stained cells per field were counted and photographed with a Nikon camera attached to the inverted phase-contrast microscope.

(2) Wound healing assays

Cells were allow to grow to confluency in 35 mm culture dishes. Three or four scratches were made within the confluent monolayer of cells using a sterile yellow plastic pipet tip. Cells were incubated at 37°C for 24 hours and photographed under a phase-contrast microscope to compare the migration of cells into the cleared area of the wound.

Histological and immunohistochemical analyses

Embryos were dissected from the deciduum and fixed in Z-FIX (Anatech Ltd, Battle Creek, MI) or (for endoderm markers) Sainte-Marie fixative (Dziadek and Adamson, 1978) for 2 hours, transferred to PBS, dehydrated, embedded in paraffin and sectioned at 5 μm onto glass slides. Some slides were processed by standard procedures and stained with hematoxylin and eosin. Paraffin-embedded sections were cleared in xylene and rehydrated through a ethanol series to PBS. Endogenous peroxidase activity was quenched by incubation of sections with 3% hydrogen peroxide in methanol for 1 hour at room temperature. The sections were then washed with PBS, blocked with 20% normal donkey serum in PBS for 2 hours at room temperature and incubated with rabbit serum against AFP or laminin (Dziadek and Adamson, 1978; Grover et al., 1983) overnight at 4°C. After washing, the sections were incubated with horseradish-peroxidase-conjugated donkey anti-rabbit Ig (Amersham Life Science, Arlington Heights, IL) diluted 1:1000, for 2 hours at 20°C or overnight at 4°C. The sections were then washed and reacted with peroxidase substrate, Vector™ SG (Vector Laboratories., Inc. Burlingame, CA). After conterstaining with Nuclear Fast Red, the sections were dehydrated and mounted.

Immunostaining of embryo outgrowth cultures was performed as follows: 5 or 6-day cultures were fixed in methanol at –20°C for 10 minutes, treated with 3% hydrogen peroxide in methanol and rehydrated through a methanol series to PBS. Cells were blocked with 20% normal goat serum (NGS) and 0.2% Triton X-100 in PBS at 4°C overnight and then incubated with a monoclonal antibody, MF20, against myosin heavy chain (MHC), or a monoclonal antibody against 165 kDa neurofilament (2H3, Developmental Studies Hybridoma Bank, Johns Hopkins University, Baltimore, MD) at 4°C overnight. After extensive washing, cells were exposed to horseradish peroxidase-conjugated goat anti-mouse IgG (Jackson ImmunoResearch West Grove, PA) diluted 1:300 in 0.2% NGS and 0.1% NP40 in PBS at 4°C overnight. Cells were washed again extensively and exposed to Vector™-SG substrate for about 5 minutes to give a black stain where positive for antigen. The reactions were stopped by washing with PBS.

RT-PCR Analysis

Poly(A)$^+$ RNA (3 μg) was isolated from embryos, treated with RNase-free DNaseI (Stratagene, San Diego, CA) and converted into cDNA using oligo(dT) as a primer.

The cDNA from pooled mutant and normal embryos was amplified by PCR using following primers: brachyury (T)-specific primers, 5′-ATCAAGGAAGGCTTTAGCAAATGGG-3′ and 5′-GAACCTC-GGATTCACATCGTGAGA-3′, which should give a 159 bp product; GATA4-specific primers, 5′-CACTATGGGCACAGCAGCTCC-3′ and 5′-TTGGAGCTGGCCTGCGATGTC-3′ which should give a 143 bp product; Mef2C-specific primers (Martin et al., 1993); cardiac αmyosin heavy chain (αMHC) and (myosin heavy chain (βMHC)-specific primers (Robbins et al., 1990); cardiac myosin light chain 2V (MLC2V)-specific primers (Miller-Hance et al., 1993); cardiac myosin light chain 2A (MLC2A)-specific primers (Kubalak et al., 1994), ANF-specific primers, 5′-CGGTGTCCAACACAGATCTG-3′ and 5′-TCTCTCGAGGTGGGTTGAC-3′, which should give a 187 bp product; desmin-specific primers, 5′-TGATGAGGCAGAT-GAGGGAG-3′ and 5′-TGAGAGCTGAGAAGGTCTGG-3′, which should give a 246 bp product; myogenin-specific primers, 5′-TGAGGGAGAGCGCAGGCTCAAG-3′ and 5′-TGCTGTCCAC-GATGGACGTAAGG-3′, which should give a 361 bp product; smooth muscle myosin heavy chain (SMHC)-specific primers, 5′-TCCATTCTGTGCACAGGTGAG-3′ and 5′-AACTTGCCA-AAGCGAGAGGTG-3′, which should give a 218 bp product; PECAM and Flk-1 (Vittet et al., 1996) and GAPDH (Hummler et al., 1996). The PCR conditions for GAPDH, brachyury (T), GATA4, Mef2C, ANF, desmin, myogenin, SMHC, PECAM and Flk-1 were performed by denaturing the DNA at 94°C for 4 minutes, followed by 35 cycles of amplification: 94°C for 25 seconds, 60°C for 30 seconds, 72°C for 1 minute and a final extension step at 72°C for 6 minutes. For αMHC, βMHC, MLC2A and MLC2V, PCR reactions were performed by denaturing the DNA at 95°C for 5 minutes, followed by 28-35 cycles of amplification: 94°C for 30 seconds, 65-70°C for 30 seconds, 72°C for 50 seconds and a final extension step at 72°C for 6 minutes. Amplified fragments were separated on a 2.0% agarose gel and visualized by staining with ethidium bromide.

RESULTS

Disruption of one *Cr1* allele in mouse embryonic stem (ES) cells

To inactivate the *Cr1* gene by homologous recombination, a

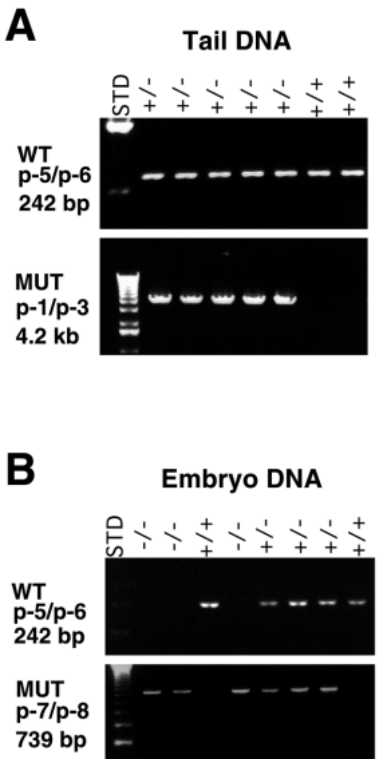

Fig. 1. Genotypes of adult mice and embryos. (A) Genotypes of adult mice were determined by PCR analysis of tail DNA using primers p-1 and p-3 to detect mutant allele (MUT) and primers p-7 and p-8 to detect wild-type (WT) allele. (B) Genotypes of embryos from *Cr1*$^{+/-}$ mating were determined by PCR analysis of embryo lysate using specific primers (p5 and 6) to detect mutant alleles (MUT) and specific primers (p7 and 8) (Xu et al., 1998) to detect wild-type (WT) alleles.

targeting vector, pCR-KO1, containing a positive selectable marker, namely bacterial neomycin-resistance gene, and a negative selectable marker, HSV tk gene, was constructed to replace exons 3, 4 and 5 (Xu et al., 1998). ES R1 cells were then electroporated with the linearized targeting vector pCR-KO1 and selected with G418 and ganciclovir. To screen for the homologous recombinant event, the DNA samples from G418-resistant ES colonies were subjected to PCR amplification using a 5′ primer, p-3, in the *neo* gene and a 3′ primer, p-1, outside the targeting vector. Ten single targeted (+/–) clones were identified and *Cr1* gene targeting was further confirmed by Southern blot analysis with a probe outside the targeting vector (Xu et al., 1998). As predicted, probe-1 gave a 5 kb band when hybridized to *Bam*HI-digested DNA from R1 wild-type cells (data not shown). The expected pattern for one native and one targeted allele (5 kb and 6.8 kb bands) occurred only in the clones identified by PCR as *Cr1*$^{+/-}$ but not *Cr1*$^{+/+}$ cells. Only the 6.8 kb band hybridized with a neo-specific probe (data not shown), indicating the absence of additional random integration events. Therefore, these ten clones have a disrupted *Cr1* in one of the two alleles.

Disruption of the *Cr1* gene in mice leads to embryonic lethality

Two independent ES *Cr1*$^{+/-}$ cell lines, E39 and E43, were microinjected into C57BL/6 blastocysts, using standard procedures, to generate 23 male chimeric mice. Most of these gave germline transmission when mated to outbred Black Swiss and to the inbred 129SvJ strain of mice. Mice derived from an additional genetic background (C57BL/6) were derived and maintained separately throughout the experiments and have generated similar results. Genotypes of mice were determined by PCR analysis of DNA extracted from tail samples (Fig. 1A). Adult heterozygous mice were apparently normal and fertile. Of the 184 progeny derived from heterozygote intercrosses in two different strains, outbred Black Swiss and inbred 129SvJ, none were homozygous mice, indicating that these mice died during gestation and that Cr1 is essential for embryonic development (Table 1A).

Table 1A. Genotypes of offspring from heterozygous matings

		Genotype*		
Genetic background	No. of mice	+/+	+/–	–/–
BlackSwiss (outbred)	134	48 (35.8%)	86 (64.2%)	0 (0%)
129SvJ (inbred)	50	20 (40.0%)	30 (60.0%)	0 (0%)
Total	184	68 (37.0%)	116 (63.0%)	0 (0%)

*Genotypes were determined by PCR analysis of tail DNA.

Table 1B. Genotypes of embryos from heterozygous matings

		Genotype*		
Stage	No. of embryos	+/+	+/–	–/–
E3.5	26	7	9	10
E6.5	12	2	6	4
E7.5-7.7	64	19	8	17 (11M)
E8.5	23	6	11	6 (6M)
E9.5	30	8	13	9 (9M)
E10.5	8	2	5	1 (1M)
E11.5	6	3	3	0
Total	169	47 (28%)	75 (44%)	47 (28%)

*Genotypes were determined by PCR analysis of tissue lysate of blastocyst outgrowths for E3.5, embryos for E6.5-8.5 and yolk sac for E9.5-11.5. M, mutated phenotype. The genetic background was BlackSwiss outbred mice.

Abnormalities in homozygous mutant embryos are apparent after developmental stage E7.5

To investigate the stage of the embryonic lethality, embryos at various stages were examined and genotyped (Fig. 1B; Table 1B). Since Cr1 is first detected in blastocysts at embryonic day 4 (E4) during development (Dono et al., 1993; Johnson et al., 1994), we analyzed early stages by collecting blastocysts at E3.5 and culturing in vitro to observe any defects in outgrowths. All blastocysts tested attached normally to the gelatin-coated dish and completely hatched from the zona pellucida after 2 days in culture. The blastocyst outgrowths were collected and genotyped after being photographed. There was no significant difference between homozygous and wild-type or heterozygous blastocysts in the proliferation of inner cell mass and the extent of trophectoderm outgrowth (Fig. 2). This indicates that Cr1 is not required at this stage of development.

All the live homozygous *Cr1*$^{-/-}$ Black Swiss and 129SvJ

embryos identified at E6.5 were morphologically normal as judged under the dissecting microscope (data not shown). Therefore, *Cr1* homozygous embryos implanted and appeared to initiate gastrulation normally. We cannot rule out that some embryos did not survive up to this stage and were resorbed.

When embryos were dissected at E7.5-7.7, most of the $Cr1^{-/-}$ embryos displayed abnormal morphology although a minority of $Cr1^{-/-}$ homozygotes were less severely affected and were still morphologically indistinguishable from normal littermates at E7.5. The embryonic region of the mutant embryos appeared distorted in shape, notched and small compared with normal littermates. The mutants were quite variable in size and shape (Fig. 3B,C).

At E8.5, all mutant embryos showed clear phenotypic defects with a small and distorted embryonic regions (Fig. 3E,F). A few resorbed sites were also observed at this stage. Genotypes of some of the resorbed embryos could not be determined due to insufficient intact embryonic material. Mutant conceptuses at E9.5 to E10.5, consisted primarily of extraembryonic tissue including yolk sacs and the developing placenta, while the embryonic region had degenerated (Fig. 3H). Mutant visceral yolk sacs (VYS) continued to enlarge from E8.5 to 9.5, but the prominent blood vessels usually present in the normal VYS were absent. We observed the same phenotypes from mice derived from two independent ES cell lines.

Histological analyses of Cr1-deficient embryos

To characterize the nature of the defect of $Cr1^{-/-}$ mutants, embryos at different stages were examined by histological analyses of fixed paraffin-embedded embryos, that were sectioned and stained with hematoxylin and eosin. As shown in Fig. 4A, the $Cr1^{+/+}$ embryos around E7.5 had generated mesodermal regions from the primitive streak that had spread through the embryos. The extraembryonic regions including the chorion, amnion, visceral and parietal endoderms were

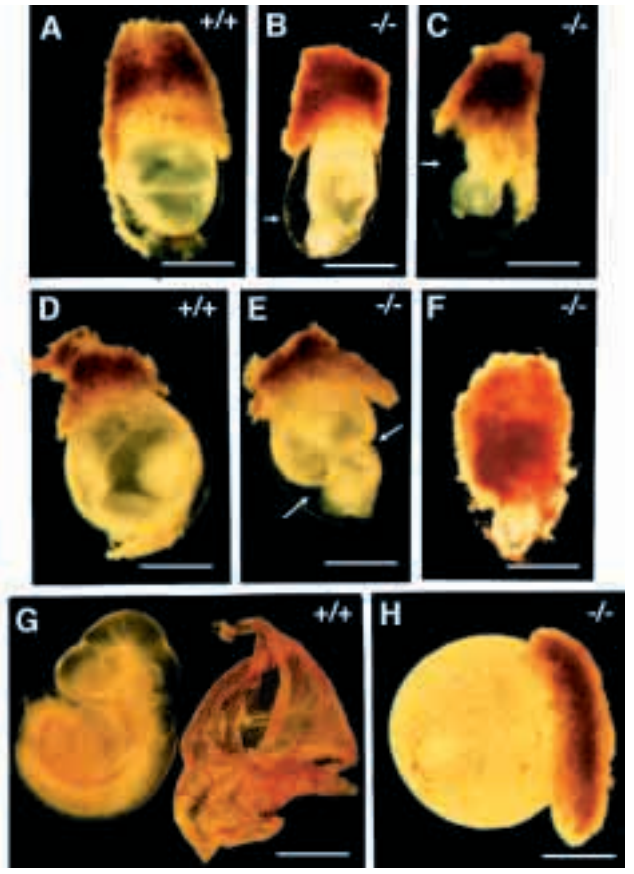

Fig. 3. Morphological analysis of normal and mutant embryos. Embryos from $Cr1^{+/-}$ mouse matings were dissected at various stages during gestation. Dissected normal embryos at E7.7 (A), E8.5 (D) and E9.5 (G) and $Cr1^{-/-}$ embryos at E7.7 (B,C), E8.5 (E,F) and E9.5 (H). There is no embryo in the visceral yolk sac in H, and note the lack of large blood vessels. Bars in A-F represent 400 μm; in G and H, 600 μm.

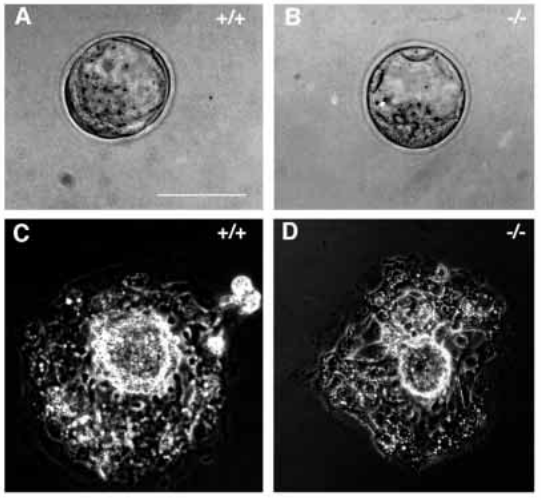

Fig. 2. Blastocyst outgrowth. E3.5 blastocysts collected from $Cr1^{+/-}$ mice mating were cultured on gelatin-coated plates, examined for proliferation and genotyped after culture. No differences between the genotypes were observed. Photographs were taken at the first day of the culture (A,B) and 3 days after the culture (C,D). Bar = 100 μm.

formed and well organized. In the mutant embryos, the three germ layers and extraembryonic structures including the visceral and parietal endoderm, trophoblastic giant cells, amnion and chorion were present but somewhat abnormal in density of staining and morphology (Fig. 4B,C). Mutant embryos had a shortened axis and the embryonic region was abnormally inflected producing a distorted neuroepithelial layer. In some cases, the neuroepithelium had formed extra folds that were filling the cavity. The presence of early mesoderm was confirmed by detection of the mesoderm marker, brachyury (T), by RT-PCR, in both $Cr^{-/-}$ and $Cr^{+/+}$ embryos (see Fig. 7). The presence of brachyury, an early mesodermal marker, is consistent with the mesoderm observed here and with its expression in embryoid bodies derived from $Cr1^{-/-}$ ES cells and the observation of differentiation of many mesodermal cell types in the mutant ES cells (Xu et al., 1998). In support of the disorganized cell layers, in situ hybridization revealed that the signal for Brachury was largely in the mid-extraembryonic region (data not shown).

Sections of the mutant embryos at E8.5 showed a severe disruption of embryonic development leading to distortion of the majority of the embryonic regions (Fig. 4E,F). Neural

epithelium could be recognized by its staining intensity but was grossly abnormal in shape. In situ hybridization analysis for the anterior neuroectoderm was widely expressed (data not shown), indicating a predominance of this tissue in homozygous mutant embryos. The mesoderm-like cells appeared abnormally compacted and lacked the matrix material seen in the normal embryos (Fig. 4E,F). In contrast, ectoderm and mesoderm in normal littermates had further differentiated into large head folds and somites (Fig. 4D).

Histological analyses of the mutant conceptuses at 9.5 days p.c. showed that yolk sacs contained extraembryonic endoderm and mesoderm (Fig. 4H). Normal and mutant embryos had similar visceral endoderm layers. Most of the mutant blood islands appeared to be small and scattered throughout the mutant yolk sac and, although red blood cells were found in mutant yolk sacs, no large blood vessels were present, in contrast to the wild-type embryo yolk sacs (Fig. 4G,H).

Analysis of some markers of extraembryonic differentiation

Sections of embryos fixed at E8.5 were stained with antibodies to alphafetoprotein (AFP) and peroxidase-labelled secondary antibodies. Staining was positive (black staining in Fig. 5) in the visceral endoderm of the VYS, and was correctly located on the outside of embryonic ectoderm in mutant embryos (Fig. 5A,B). This secreted glycoprotein is a specific product of the visceral endoderm only, at this stage of development. The parietal endoderm of mutant embryos stained strongly with antibodies to laminin (Fig. 5C,D), showing that these two extraembryonic endodermal tissues were normal, as suggested by the hematoxylin- and eosin-stained sections in Fig. 4. Weak staining for laminin was visible in other tissues of mutant embryos.

Assays for markers of cardiogenesis and vasculogenesis

Two types of approaches were used to detect defective tissue development. One was to culture embryos in vitro so that any cardiomyocytes in the embryos would have time to form rhythmically contracting masses of cells that could be identified further as cardiac myocytes. Even after extended culture, no beating aggregates of cells were ever seen in mutant embryo cultures, whereas, beating was prominent in wild-type cultures. Table 2 summarizes the numbers of embryos that were observed and the numbers of embryos that were defective in cardiogenesis. These results were confirmed by staining fixed cultures with an antibody to myosin heavy chain. No staining was observed in mutant cultures (Fig. 6A,B). When the cultures were disaggregated with collagenase and replated, cultures grew many aggregates of rounded cells that extended axon-like structures. These stained with antibody (MF20) to neurofilament protein, confirming that both wild-type and mutant embryos differentiated equally well to neurons (Fig. 6C,D).

The second type of assay was the detection and semiquantification of several mRNAs that are specific to cardiovascular tissues. Individual embryos on day E8.5-8.7 were genotyped and pooled into $Cr1^{-/-}$ and $Cr1^{+/+}$ types for comparisons. RNA preparations were subjected to RT-PCR to probe for several tissue-specific markers that have been described in the literature. The cDNAs were examined in a 10-fold dilution series to ensure that the linear range of amplified cDNA was used and to compare the levels of mRNA in normal and mutant embryos. Fig. 7 shows a compilation of the results. The early expressing transcription factors brachyury (T), GATA4 and MEF2C were expressed in both normal and mutant embryos. In addition, eHAND and dHAND cardiogenic transcripition factors were also expressed in wild-type and homozygous mutant embryos (data not shown). Myogenin, specific for skeletal muscle differentiation, was weak but positive in mutant embryos. In contrast, five cardiac-specific marker genes remained unexpressed in mutant embryos: α- and β-myosin heavy chains (MHC); myosin light chains 2A and 2V; atrial natriuretic factor (ANF) were all absent in $Cr1^{-/-}$ embryos but present in wild type (Fig. 7).

Since large blood vessels were absent from the visceral yolk sacs of mutant embryos, we also tested for markers of endothelial cells, such as the growth factor receptors Flk-1, Flt-1, Tie-1 and Tie-2, as well as PECAM, an adhesion protein. Flk-1 is necessary for visceral endothelial cell development (Shalaby et al., 1995) and is detected as one of the earliest markers of endothelium. PECAM and tie-1 expression follow

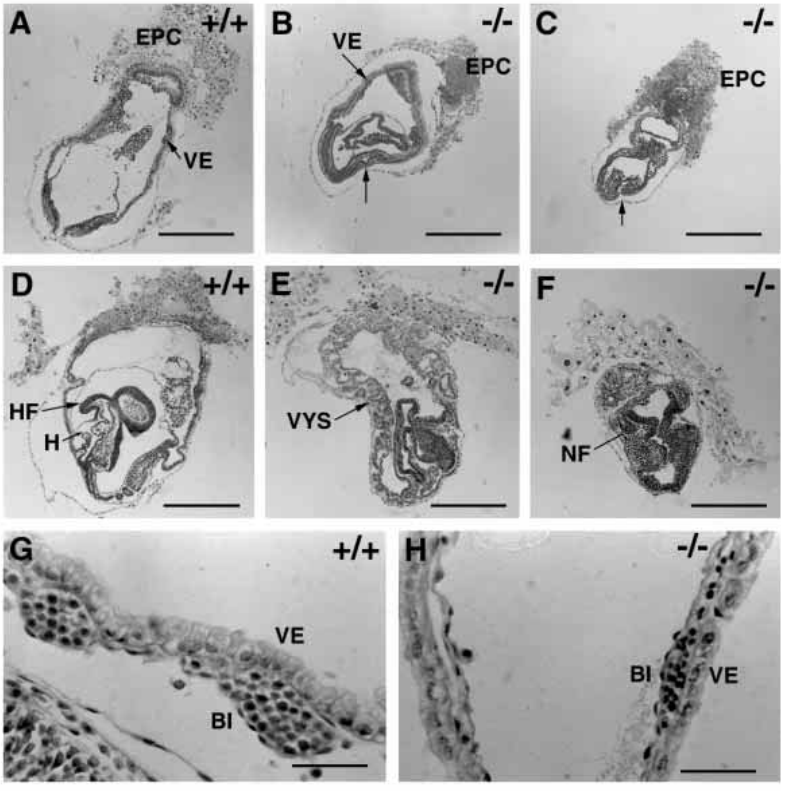

Fig. 4. Histological analysis of normal and mutant embryos. Sagittal sections of embryos at E7.7 (A-C), E8.5 (D-F) and E9.5 (G,H). Normal embryos at E7.7 (A), E8.5 (D) and E9.5 (G). All stained with hematoxylin and eosin. BI, blood island; EPC, ectoplacental cone; H, heart; HF, head-folds; NF, neural fold; VE, visceral endoderm; VYS, visceral yolk sac. Unlabeled arrows denote abnormal morphology. Bars in A-F represent 350 μm; in G and H, 175 μm.

Table 2 Formation of beating cardiomyocytes and neurons in embryo culture

Stages	No. of embryos	No. of embryos that form neurons	No. of embryos that form cardiomyocytes
E7.7 +/+	5	ND*	5 (100%)
E7.7 +/–	8	ND	8 (100%)
E7.7 –/–	6	ND	0 (0%)
E8.5 +/+	6	6 (100%)	6 (100%)
E8.5 +/–	9	9 (100%)	9 (100%)
E8.5 –/–	4	4 (100%)	0 (0%)

*Not done.

soon after (Vittet et al., 1996). The VEGF receptor, Flk-1, was expressed, as was tie-2 (observed in sections of E8.5 embryos using immunostaining, data not shown). The adhesion molecule PECAM is restricted to endothelial cells at this stage and was found to be expressed in mutant embryos. The muscle intermediate filament protein, desmin, and the smooth muscle-specific myosin heavy chain (SMHC) (Drab et al., 1997) were also expressed (Fig. 7). The cDNA amplified by the SMHC primers was further tested by digestion with *Ava*II, to which it was resistant, indicating that vascular smooth muscle rather than the intestinal isoform was expressed (Drab et al., 1997). Markers of hemoglobins were detected by RT-PCR (data not shown) in all embryos at E8.5, including globins βH1 and ε^{y}. The amounts of RNA present in each of the samples was similar (Fig. 7), as denoted by the results of RT-PCR assays on GAPDH gene expression (Hummler et al., 1996). In summary the tissues that were absent in *Cr1* null embryos were cardiac tissues. While differentiation of endothelial and smooth muscle cells occurred, we know that the morphogenesis of tissues from these cells was not completely normal because large blood vessels were absent from the visceral yolk sac (Fig. 3H).

The lethal phenotype can be rescued in chimeric mice

When the heart fails to beat during development, the circulation of nutrients is inadequate, the embryo dies and the contribution of specific gene functions in later tissues and organs cannot be determined. In order to test if the development of the *Cr1* null embryo can be rescued by the presence of normal embryo cells, chimeric embryos were constructed as follows. ES cells with one disrupted *Cr1* gene were subjected to a further round of gene targeting using vector 2. Electroporation of two of the single KO cell lines with this vector, produced many clones that were isolated and four of these were expanded. These lines were karyotyped and one was chosen for microinjection into blastocysts derived from the C57Bl6 mouse. The two mouse strains, 129Sv and C57Bl6 have a different isoform of the enzyme glucose phosphoisomerase (GPI) that migrate at different rates during cellulose acetate electrophoresis. The composition of the resulting chimeric tissues in the mosaic mice produced in this way can be estimated by densitometry of the stained bands on the agarose overlay containing enzyme. The mixture of $Cr1^{-/-}$ ES cells and wild-type embryonic embryos gave rise to normal embryos that were analyzed on day E14.5 and young pups were analyzed at 10 days after birth. The results are summarized in Table 3, where each line represents the % mutant cell contribution as an average of all individual embryos and for each tissue. The tissues in mosaic animals all contained a contribution from mutant cells, that was approximately 50% for each embryo, indicating that for that particular proportion of ES cells in an embryo, the cells were able to make a similar contribution to all the tissues. In other words, mutant ES cells were able to differentiate into all tissues and the normal cells were able to make a complete rescue of the previously mutant phenotype. Since Cr1 is a secreted protein, this result indicates that a paracrine influence of the Cr1 protein on $Cr1^{-/-}$ cells is sufficient to restore normal function.

The effect of Cr1 abrogation on mouse embryo-derived fibroblasts (MEFs)

To test for differences in cell behavior that might explain the developmental consequences of *Cr1* gene abrogation, fibroblast cell lines were isolated from disaggregated E8.5 embryos, as described in the Materials and Methods section. We first tested if the loss of *Cr1* expression affected the growth rate of MEFs in the MTT proliferation assay. The growth of $Cr1^{-/-}$ MEFs was 50.3±8.1% of the rate of the wild-type MEFs (Fig. 8A). This result confirmed that there is a growth deficit in early differentiated embryonic mesoderm cells in the absence of Cr1 expression.

In monolayer wound healing assays, wild-type cells migrated into and filled the gap made in the monolayer cultures of MEFs in 24 hours, whereas in the same period, very little migration was observed in the wounded $Cr1^{-/-}$ MEFs (Fig. 8B). This was not caused by the higher rate of proliferation in wild-type MEFs because the 24 hour migration time was insufficient for one cell division. In the first 24 hours after seeding, wild-type MEFs have increased by 38%, while $Cr1^{-/-}$ cells have increased 20% (data from Fig. 8A), growth rates that cannot explain the difference in the wound healing.

The morphology of the tissues in mutant embryos suggests that cell-matrix distributions are aberrant. We tested MEFs for evidence of differences in cell migration towards a set of purified matrix proteins using haptotactic assays, as described in the Materials and Methods. Wild-type MEFs were able to migrate better than mutant cells towards fibronectin and

Table 3 Chimeric mouse analysis

Tissues*	% $Cr1^{-/-}$ ES contribution	
	E14.5 embryos	10d neonates
Yolk sac	45.0±1.8	–
Limb	50.0±1.4	–
Blood	48.4±5.0	58.3±15.5
Brain	46.3±0.7	55.3±10.1
Gut	49.7±0.1	33.7±9.0
Heart	48.3±0.6	64.0±23.4
Liver	48.6±0.9	48.9±9.8
Lung	46.6±1.9	49.3±12.7
Muscle	–	62.7±11.7
Kidney	–	59.2±14.1
Spleen	–	40.8±16.5

*Tissues from chimeric mice constructed from $Cr1^{-/-}$. ES cells and C57BL/6 blastocysts were analyzed at two stages. Each result represents average ± standard deviation of the percentage of ES cell contribution for tissues from 4 embryos or animals.

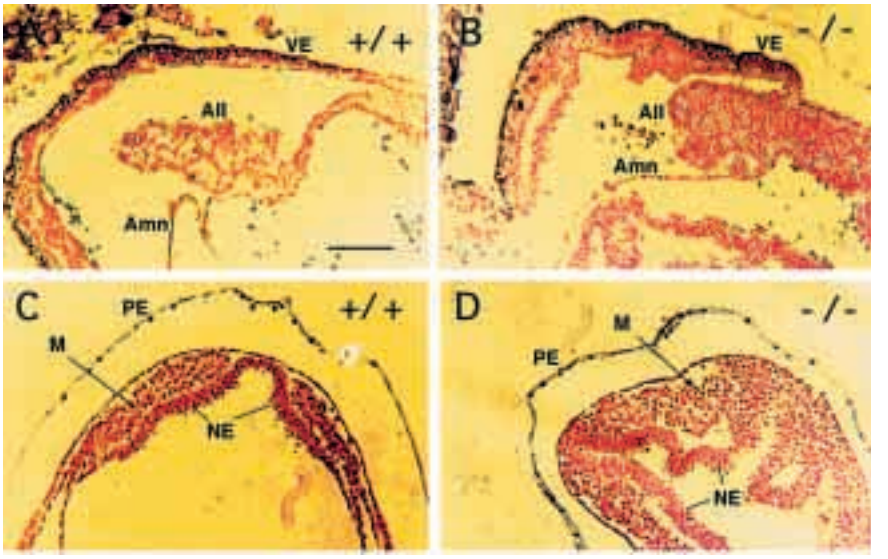

Fig. 5. Marker expression in the yolk sacs and embryos. Markers of endoderm expression in E8.5 embryos. (A,B) Anti-AFP reactions stained the visceral extraembryonic endoderm (VE) (black) in both *Cr1*$^{+/+}$ and *Cr1*$^{-/-}$ embryos. (C,D) Anti-laminin reacted with the parietal endoderm (PE) of both normal and mutant embryos similarly. All, allantois; Amn amnion; M, mesoderm; NE, neuroepithelium. Bar, 100 μm.

collagens I and IV, while on laminin, the mutant MEFs had much greater migratory activity compared to the wild-type cells (Fig. 9A). The quantification of this assay (Fig. 9B) shows striking differences between the motility of the mutant MEFs, which moved 9-fold faster on laminin, but 5-fold *slower* on fibronectin, 9-fold *slower* on collagen I and almost equally as fast as wild-type cells on Collagen IV.

In view of the different activities of the wild-type and mutant MEFs in migrating over matrix substrata, we tested the relative adhesion of the cells to the same matrix molecules in 96-well attachment assays. Fig. 10 shows that the *Cr1*$^{-/-}$ MEFs had a reduced capacity to attach to all the matrix components tested, although they adhered to laminin best (71% of wild-type). These assays suggest that the cell *populations* that make up the heterogenous cells established from wild-type and *Cr1*$^{-/-}$ embryos are different and cannot be directly compared. However, these studies tell us that the viable cells in a mutant E8.5 embryo have reduced adhesion to matrix, reduced overall growth rates, reduced capacity to migrate over fibronectin and reduced wound healing capacity compared to the cells in a wild-type embryo. These differences in the characters of the MEFs from wild-type and mutant embryos explain on the cellular level, how the aberrant morphological development of *Cr1*$^{-/-}$ embryos occurs.

DISCUSSION

In summary, we have shown here that the growth factor Cr1, plays a crucial role in early mouse development. The most obvious molecular manifestation of the lack of *Cr1* expression in developing embryos is the lack of all cardiac-specific gene expression. Thus functional cardiomyocytes fail to form, no rhythmic contractions occur and embryo development ceases. But developmental defects are seen also in other tissues starting during gastrulation, when the E7.5 *Cr1*$^{-/-}$ egg cylinder begins to embark on aberrant morphogenesis. This is visible as small embryo size and abnormal dents and folds in the egg cylinder. Upon sectioning, it is observed that the neuroepithelium has not formed a smooth fold and never forms a tube, events summarized as defects in anteroposterior axis formation. The embryonic mesoderm is defective while the extraembryonic tissues develop relatively well. The trophoblast, amnion, allantois, parietal endoderm and visceral endoderm are well represented in *Cr1*$^{-/-}$ embryos at

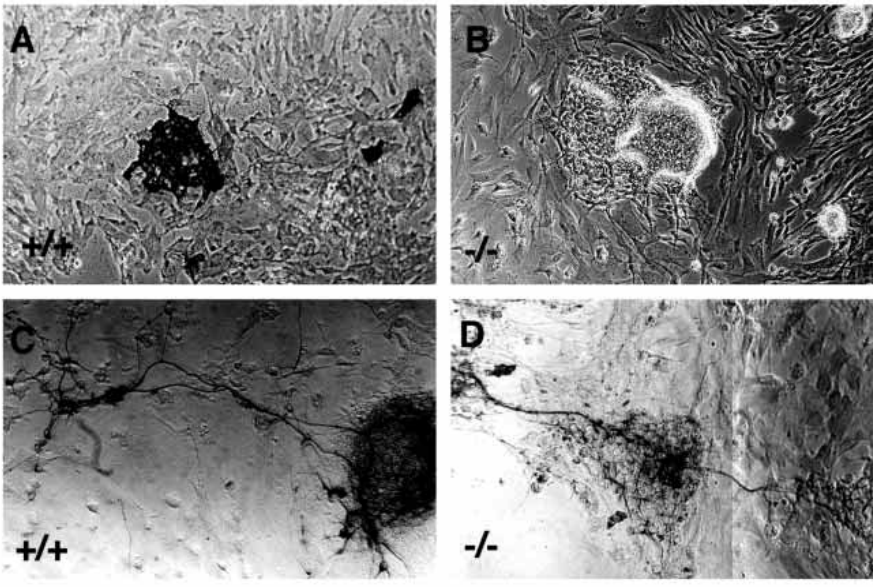

Fig. 6. Embryo culture and immunostaining. (A,B) E8.5 embryos were cultured as described in the Materials and Methods section, and fixed after 5 days when rhythmic beating was observed only in the wild-type (A) cultures. Immunostaining with antibody to myosin heavy chain confirmed that only wild-type embryos were expressing myosin. (C,D) Embryo cultures were replated and cultured for 6 more days when neuron-like structures were observed in wild-type (C) and and mutant (D) cultures. Immunostaining for neurofilament protein confirmed the identification of nerve cells.

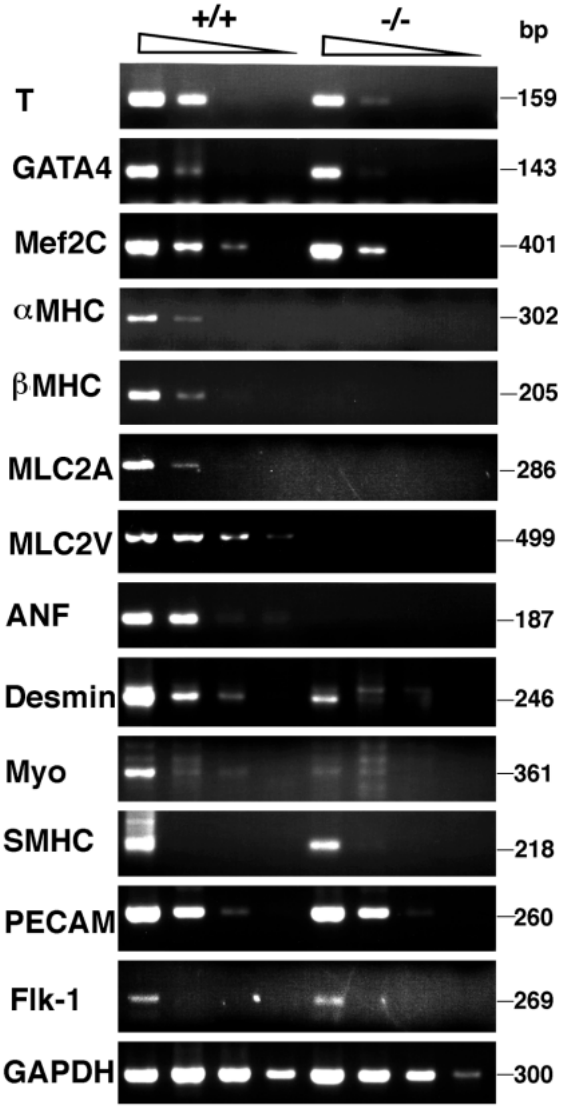

Fig. 7. Semi-quantitation of markers by RT-PCR analysis. mRNA was isolated from E8.7 embryos pooled into wild-type and mutant groups, and subjected to RT-PCR using gene-specific primers as described in the Methods section. Samples of cDNA and three 10-fold dilutions were analyzed to compare the levels of gene expression. Only the myosin and ANF genes were not expressed in the $Cr1^{-/-}$ embryos. See text for explanation of genes tested.

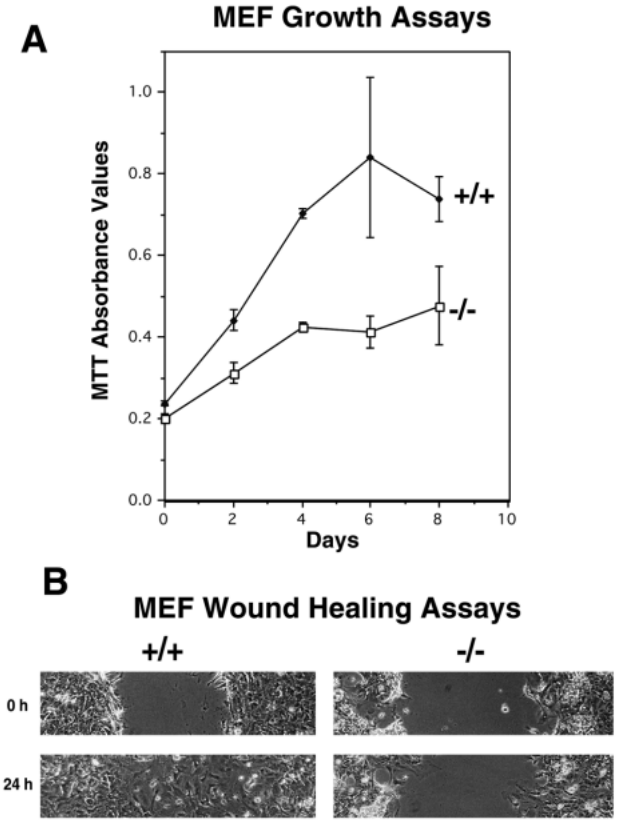

Fig. 8. Growth and migration of MEFs derived from wild-type $Cr^{+/+}$ and $Cr^{-/-}$ embryos. (A) Growth of MEFs measured by the MTT assay (Promega) shows mutant cells grow at 50% of the rate of wild-type cells. (B) Phase-contrast micrographs of wounds in monolayers of MEFs from $Cr^{+/+}$ and $Cr^{-/-}$ MEFs, showed the poor migration of mutant cells in 24 hours of culture, in contrast to wild-type cells.

E8.5 and appear to be as abundant as in wild-type embryos. This was true for two of the three strains of mice (Swiss Black and 129SvJ) that were examined in sufficient detail.

After this paper was submitted for publication, another study involving the abrogation of *cripto1* in mouse came to our attention (Ding et al., 1998). The phenotype of homozygous embryos obtained for this *lacZ*-containing targeting vector was identical to that described here, with a very similar range of variation obtained in a Black Swiss background. These workers made an elegant analysis of embryonic marker aberrances, including HNF3-β, Shh, Mox1, BF1, En1, Krox20, HoxB1, Fgf8, Lim1, Gsc, Hesx1, Hex1 and Cer1, in addition to some of the markers analyzed here. Their study complements and supports our results, and also suggests the nature of the aberrancy in $Cripto^{-/-}$ embryos that prevents the formation of the anteroposterior axis of the embryo.

Three major roles for Cr1 during development

Our results suggest at least three roles for Cr1 during development. One is that Cr1 is needed to produce the correct number and specification of embryonic precursor cells, because although all three germ layers are represented, not all cell types appear. The E7.7 mutant embryos are already smaller than normal and we showed that cells derived from mutant E8.5 embryos (MEFs) have reduced cell proliferation rates. However, we could detect no differences in the rates of proliferation of ES $Cr1^{-/-}$ or ES wild-type cells (data not shown), and we could not detect any significant difference in the cells growing out from the blastocysts of Cr1-positive or -negative preimplantation embryos (Fig. 2). The observations here indicate that changes in proliferation rates of mutant embryo cells occur between E6.5 and E7.7. We have also measured a lower growth rate in F9 $Cr1^{-/-}$ embryonal carcinoma cells compared to wild-type F9 of about 25% (data not shown, note that F9 cells are partially differentiated; Adamson et al., 1981). It has been reported that the human embryonic carcinoma cell line, NTera/2D, grows at a reduced rate in the presence of antisense to Cr1 (Baldassarre et al.,

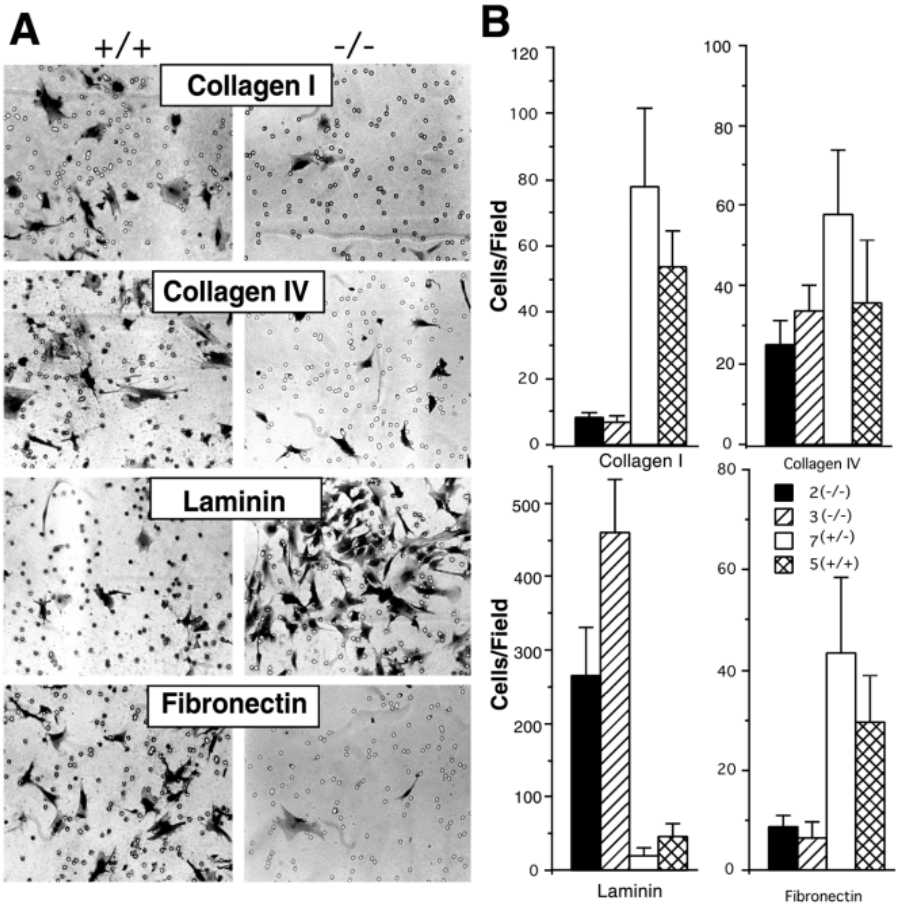

Fig. 9. Migration (haptotactic) assays of MEFs over different substrata coating the undersurface of membranes in Boyden chamber assays. (A) Cultures of $Cr^{-/-}$ MEFs derived from two different embryos were tested and compared with two different wild-type and heterozygous MEF cultures. The cells that migrated through the membrane were fixed and stained and counted. (B) Quantification of the results of three experiments similar to that shown in A. Mutant MEFs have a strong attraction towards laminin, while wild-type cells favor fibronectin and collagen I.

1996). We have also noted the reduced proliferation of mouse mammary cells when a Cr1 antisense vector is expressed in the cells and increased growth when Cr1 is overexpressed (Niemeyer et al., 1998). Thus, the evidence for a role for Cr1 in the growth regulation of several specific cell types is well established.

A second role for Cr1 is to give a *spatial* signal that is required for morphogenesis of cell layers, observed in null embryos as distorted neuroepithelia and incorrect placement of mesoderm cells. The anteroposterior axis of the embryo is not formed in *Cr1* null embryos. Perhaps one role of Cr1 is to form a morphogenic gradient across the embryonic field, with a high concentration in the mesodermal cells of the primitive streak. Perhaps other cell types such as those from the neuroepithelium migrate towards the Cr1-producing mesoderm in a chemotactic fashion, in order to shape or maintain the tissue layers for morphogenesis. We showed that MEFs derived from mutant embryos have reduced migratory activity in two different assays (Figs 8B, 9), as well as reduced adhesivity for matrix components (Fig. 10). Whether these cell types represent different cell populations is not at issue, but they do illustrate that the cells of the mutant embryo have different interactive properties that explain the altered developmental pathways of $Cr1^{-/-}$ embryos.

No cardiogenesis in *Cr1*$^{-/-}$ embryos

The *Cr1* null embryo has aberrant morphology from at least as early as E7.7, when the heart-producing mesoderm field is normally starting to form a tube (Fishman and Chien, 1997). Hence the third defect is that the Cr1 null embryo never forms any cells that express the cardiac myosin genes (Fig. 7) and therefore no *functional* heart cells develop. It remains to be established if this effect is a consequence of earlier deficits in the numbers or the location of a fraction of mesoderm cells designated as precardiomyocytes. A critical mass or placement of this putative group of precursor cells may be required for cardiomyocyte induction and differentation. Further work will be needed to determine whether Cr1 acts at the early stage and/or in the process of cardiomyocyte differentiation itself, or at several points in between. It is also possible that the deficit in vascularization of the visceral yolk sac that we observed in mutant embryos is a fourth defect, but because we detected the expression of several endothelial and smooth muscle cell marker genes, this will have to be analyzed further using other approaches.

The lack of activation of the cardiac myosin genes in the absence of Cr1 is currently being studied further at the molecular level. The use of the ES cell system and the in vitro cardiac differentiation model is useful in dissecting the molecular mechanisms underlying the activation of myosin genes by Cr1. In the doubly targeted ES cell system, the removal of the growth factor LIF stimulates differentiation. This can be observed as aggregates of cells called embryoid bodies and as teratocarcinomas that differentiate as subcutaneous tumors in the adult animal. In this model, we showed that a large range of tissues including ectodermal, endodermal and mesodermally derived tissues were produced from $Cr^{-/-}$ ES cells. Only cardiomyocytes were never detected

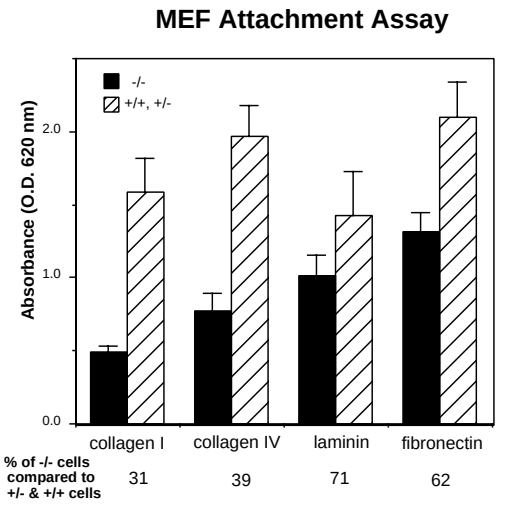

Fig. 10. Adhesion of MEFs to matrix substrata in attachment assays. The black bars represent averages of 3 wells of mutant MEFs and the hatched bars represent 6 wells of control MEFs. The $Cr^{-/-}$ MEFs adhere less well to all substrata but adhesion to laminin is the highest. The averaged percentage adhesion of mutant cells compared to wild-type cells is shown below the graph.

(Xu et al., 1998). Whether *pre*cardiomyocytes are absent from the Cr1 null embryo is a more difficult question, but might be tested using the ES cell model. We predict that cardiomyoblasts that have started to express cardiac myosin genes but have not yet started to contract, are absent from $Cr1^{-/-}$ embryos, because no myosin gene transcripts were detected.

Extraembryonic, neuroepithelium and vascular tissues develop in $Cr^{-/-}$ embryos

In spite of the deficit in morphogenesis and cardiogenesis in *Cr1* null embryos, we have ascertained that the differentiation of neuroepithelium proceeds and that endothelial and smooth muscle cells differentiate. The extraembryonic tissues develop well and cell-type-specific marker expression indicates that hematopoiesis and vasculogenesis both occur, and allow us to conclude that at least the hemangioblast precursor cells (Auerbach et al., 1997; Risau et al., 1988) that give rise to these specialized tissues are produced normally. It may not be surprising then that, if Cr1 is reintroduced into the earliest stage of embryogenesis before Cr1 is needed, the abnormal development is rescued (Table 3). This was achieved by constructing chimeric animals from normal and $Cr1^{-/-}$ cells. We conclude that the rescue occurs because Cr1 is a soluble secreted growth factor that can therefore act in a paracrine fashion on $Cr1^{-/-}$ cells. This result implies that receptors are present on some embryonic cells at the crucial time when Cr1 is needed for development. This time may be revealed after the cloning of the receptor (not so far achieved), or by examining the activation of new genes during the early stages of embryogenesis from E7.0 to E8.5.

The question of the place in the signaling pathways that is held by Cr1 is important. It is clear that Cr1 acts upstream of myosin gene activation, but appears to be independent of the pathways involving the important cardiogenic transcription factors Nkx2.5 (Lints et al., 1993); GATA4 (Molkentin et al., 1997); MEF2C (Edmondson et al., 1994; Lin et al., 1997); eHAND and dHAND (Biben and Harvey, 1997; Cserjesi et al., 1995; Srivastava et al., 1997) reviewed in (Lyons, 1996; Olson, 1997; Olson and Srivastava, 1996). These transcription factors are all expressed in $Cr^{-/-}$ embryos (Fig. 8) and differentiating ES cells (Xu et al., 1998). It might now be instructive to determine the status of Cr1 expression in the embryos that have abrogated *Nkx2.5*, *GATA4* or *MEF2C* genes. The myosin genes are activated by a number of transcription factors, but only serum response factor (SRF) seems to be a logical target for Cr1, being a growth factor. The fact that Cr1 addition to receptive cells, activates the Ras/Raf/ MAPK pathway (Kannan et al., 1997) supports this suggestion and awaits testing.

A further implication is that if Cr1 can influence receptive cells to switch to a cardiogenesis program, there may be a means to treat patients with deficits of cardiac cells due to anoxia and cell death. We have as yet been unable to rescue the $Cr^{-/-}$ ES cell differentiating in vitro, by the addition of soluble recombinant Cr1. This is probably because the concentration or conformation of the exogenous Cr1 is incorrect and the cells must be at the receptive state to achieve this end. Finding such conditions for cardiogenic induction by Cr1 would be an important first step in translating these findings to a clinical setting.

The *Cr1* gene is a member of a growing family, called the CFC family identified in mouse, frog and zebrafish (Kinoshita et al., 1995; Shen et al., 1997; Zhang et al., 1998). The human homologue of Cr1 in mouse differs in one important respect; it does not have an obvious amino-terminal signal sequence for secretion. Otherwise, the homology is high overall. The *cryptic* gene, also expressed in mouse and related in pattern to Cr1, has a similar but distinct tissue expression during development and is unlikely to be able to compensate for the loss of Cripto expression (Shen et al., 1997). Recently, a similarly related, but not homologous gene (22-32% homology) was identified in zebrafish and this also is required during gastrulation (Zhang et al., 1998). This family of genes appears to be important in the early stages of development and may provide a large increment in our understanding of complicated multigene processes such as gastrulation and the early specification of tissues and organs. In the case of Cr1, the data here suggest roles in stimulating the growth of certain embryo cells and in cell-matrix interactions, and also suggest a contribution to directed cell migrations and the regulation of the appearance of cardiac precursor cells during morphogenesis.

We are grateful for critical comments on the manuscript from Drs H. Baribault, R. G. Oshima, and C. Macleod. Grant support from the Department of Defense, grant number DAMD17-94-J-4286 (to E.D.A.) and from the Italian Association for Cancer (AIRC) (to M.G.P.) is gratefully acknowledged. This work was done during the tenure of a research fellowship (97-71) from the Americal Heart Association, California Affiliate (to C. X).

REFERENCES

Adamson, E. D., Deller, M. J. and Warshaw, J. B. (1981). Functional EGF receptors on embryonic cells. *Nature* **291,** 656-659.

Auerbach, R., Gilligan, B., Lu, L. S. and Wang, S. J. (1997). Cell interactions in the mouse yolk sac – vasculogenesis and hematopoiesis. *J. Cell. Physiol.* **173,** 202-205.

Baldassarre, G., Bianco, C., Tortora, G., Ruggiero, A., Moasser, M.,

Dmitrovsky, E., Bianco, A. R. and Ciardiello, F. (1996). Transfection with a CRIPTO anti-sense plasmid suppresses endogenous CRIPTO expression and inhibits transformation in a human embryonal carcinoma cell line. *Int J Cancer* **66,** 538-543.

Biben, C. and Harvey, R. P. (1997). Homeodomain factor Nkx2-5 controls left/right asymmetric expression of bHLH gene eHAND during murine heart development. *Genes Dev.* **11,** 1367-1369.

Bradley, A. (1987). Production and analysis of chimaeric mice. In *Teratocarcinomas and Embryonic Stem Cells: a Practical Approach* (ed. E. J. Robertson), pp. 113-151. Oxford: IRL Press.

Brandt, R., Normanno, N., Gullick, W. J., Lin, J.-H., Harkins, R., Scheider, D., Jones, B.-W., Ciardiello, F., Persico, M. G., Armenante, F., Kim, N. and Salomon, D. S. (1994). Identification and biological characterization of an epidermal growth factor-related protein: Cripto-1. *J. Biol. Chem.* **269,** 17320-17328.

Ciccodicola, A., Dono, R., Obici, S., Simeone, A., Zollo, M. and Persico, M. G. (1989). Molecular characterization of a gene of the 'EGF family' expressed in undifferentiated human NTERA2 teratocarcinoma cells. *EMBO J.* **8,** 1987-1991.

Cserjesi, P., Brown, D., Lyons, G. E. and Olson, E. N. (1995). Expression of the novel basic helix-loop-helix gene eHAND in neural crest derivatives and extraembryonic membranes during mouse development. *Dev. Biol.* **170,** 664-678.

Ding, J., Yang, Y., Yan, Y.-T., Chan, A., Desai, N., Wynshaw-Boris, A. and Shen, M. M. (1998). Cripto is required for correct orientation of the anterior-posterior axis in the mouse embryo. *Nature* **395**, 702-707.

Dono, R., Montuori, N., Rocchi, M., De Ponti-Zilli, L., Ciccodicola, A. and Persico, M. G. (1991). Isolation and characterization of the CRIPTO autosomal gene and its X-linked related sequence. *Amer. J. Hum. Genet.* **49,** 555-565.

Dono, R., Scalera, L., Pacifico, F., Acampora, D., Persico, M. G. and Simeone, A. (1993). The murine cripto gene: expression during mesoderm induction and early heart morphogenesis. *Development* **118,** 1157-1168.

Drab, M., Haller, H., Bychkov, R., Erdmann, B., Lindschau, C., Haase, H., Morano, I., Luft, F. C. and Wobus, A. M. (1997). From totipotent embryonic stem cells to spontaneously contracting smooth muscle cells: a retinoic acid and db-cAMP in vitro differentiation model. *FASEB J.* **11,** 905-915.

Dziadek, M. A. and Adamson, E. D. (1978). Localization and synthesis of alphafetoprotein in post-implantation mouse embryos. *J. Embryol. Exp. Morph.* **43,** 289-313.

Edmondson, D. G., Lyons, G. E., Martin, J. F. and Olson, E. N. (1994). Mef2 gene expression marks the cardiac and skeletal muscle lineages during mouse embryogenesis. *Development* **120,** 1251-1263.

Fishman, M. C. and Chien, K. R. (1997). Fashioning the vertebrate heart: earliest embryonic decisions. *Development* **124,** 2099-2117.

Grover, A., Oshima, R. G. and Adamson, E. D. (1983). Epithelial layer formation in differentiating aggregates of F9 embryonal carcinoma cells. *J. Cell. Biol.* **96,** 1690-1696.

Hogan, B. L. M., Costantini, F. and Lacy, E. (1993). *Manipulating the Mouse Embryo: A Laboratory Manual*. Cold Spring Harbor, NY: Cold Spring Harbor Laboratories.

Hummler, E., Barker, P., Gatzy, J., Beermann, F., Verdumo, C., Schmidt, A., Boucher, R. and Rossier, B. C. (1996). Early death due to defective neonatal lung liquid clearance in alpha-ENaC-deficient mice. *Nat. Genet.* **12,** 325-328.

Johnson, S. E., Rothstein, J. L. and Knowles, B. B. (1994). Expression of epidermal growth factor family gene members in early mouse development. *Dev. Dyn.* **201,** 216-226.

Kannan, S., De Santis, M., Lohmeyer, M., Riese, D. J., Smith, G. H., Hynes, N., Seno, M., Brandt, R., Bianco, C., Persico, G., Kenney, N., Normanno, N., Martinez-Lacaci, I., Ciardiello, F., Stern, D. F., Gullick, W. J. and Salomon, D. S. (1997). Cripto enhances the tyrosine phosphorylation of Shc and activates mitogen-activated protein kinase (MAPK) in mammary epithelial cells. *J. Biol. Chem.* **272,** 3330-3335.

Kinoshita, N., Minshull, J. and Kirschner, M. W. (1995). The identification of two novel ligands of the FGF receptor by a yeast screening method and their activity in Xenopus development. *Cell* **83,** 621-630.

Kubalak, S. W., Miller-Hance, W. C., O'Brien, T. X., Dyson, E. and Chien, K. R. (1994). Chamber specification of atrial myosin light chain-2 expression precedes septation during murine cardiogenesis. *J. Biol. Chem.* **269,** 16961-16970.

Liguori, G., Tucci, M., Montuori, N., Dono, R., Lago, C. T., Pacifico, F., Armenante, F. and Persico, M. G. (1996). Characterization of the mouse Tdgf1 gene and Tdgf pseudogenes. *Mamm. Genome* **7,** 344-348.

Lin, Q., Schwarz, J., Bucana, C. and Olson, E. N. (1997). Control of mouse cardiac morphogenesis and myogenesis by transcription factor Mef2c. *Science* **276,** 1404-1407.

Lints, T. J., Parsons, L. M., Hartley, L., Lyons, I. and Harvey, R. P. (1993). Nkx-2.5: a novel murine homeobox gene expressed in early heart progenitor cells and their myogenic descendants. *Development* **119,** 419-431.

Lyons, G. E. (1996). Vertebrate heart development. *Curr. Opin. Genet. Dev.* **6,** 454-460.

Mansfield, P. J. and Suchard, S. J. (1994). Thrombospondin promotes chemotaxis and haptotaxis of human peripheral blood monocytes. *J. Immunol.* **153,** 4219-4229.

Martin, J. F., Schwarz, J. J. and Olson, E. N. (1993). Myocyte enhancer factor (MEF) 2C: a tissue-restricted member of the MEF-2 family of transcription factors. *Proc. Natl. Acad. Sci. USA* **90,** 5282-5286.

Miller-Hance, W. C., LaCorbiere, M., Fuller, S. J., Evans, S. M., Lyons, G., Schmidt, C., Robbins, J. and Chien, K. R. (1993). In vitro chamber specification during embryonic stem cell cardiogenesis. Expression of the ventricular myosin light chain-2 gene is independent of heart tube formation. *J. Biol. Chem.* **268,** 25244-25252.

Molkentin, J. D., Lin, Q., Duncan, S. A. and Olson, E. N. (1997). Requirement Of the Transcription Factor Gata4 For Heart Tube Formation and Ventral Morphogenesis. *Genes Dev.* **11,** 1061-1072.

Niemeyer, C. C., Persico, M. G. and Adamson, E. D. (1998). Cripto: roles in mammary cell growth, survival, differentiation and transformation. *Cell Death Differ.* **5,** 440-449.

Olson, E. N. (1997). Things are developing in cardiology. *Circ. Res.* **80,** 604-606.

Olson, E. N. and Srivastava, D. (1996). Molecular pathways controlling heart development. *Science* **272,** 671-676.

Risau, W., Sariola, H., Zerwes, H. G., Sasse, J., Ekblom, P., Kemler, R. and Doetschman, T. (1988). Vasculogenesis and angiogenesis in embryonic-stem-cell-derived embryoid bodies. *Development* **102,** 471-478.

Robbins, J., Gulick, J., Sanchez, A., Howles, P. and Doetschman, T. (1990). Mouse embryonic stem cells express the cardiac myosin heavy chain genes during development in vitro. *J. Biol. Chem.* **265,** 11905-9.

Robertson, E. J. (1987). Embryo-derived stem cell lines. In *Teratocarcinomas and Embryonic Stem Cells: a Practical Approach* (ed. E. J. Robertson), pp. 71-112. Oxford: IRL Press, Inc.

Shalaby, F., Rossant, J., Yamaguchi, T. P., Gertsenstein, M., Wu, X. F., Breitman, M. L. and Schuh, A. C. (1995). Failure of blood-island formation and vasculogenesis in Flk-1-deficient mice. *Nature* **376,** 62-66.

Shen, M. M., Wang, H. and Leder, P. (1997). A differential display strategy identifies Cryptic, a novel EGF-related gene expressed in the axial and lateral mesoderm during mouse gastrulation. *Development* **124,** 429-442.

Srivastava, D., Thomas, T., Lin, Q., Kirby, M. L., Brown, D. and Olson, E. N. (1997). Regulation Of Cardiac Mesodermal and Neural Crest Development By the Bhlh Transcription Factor, dHand. *Nature Genetics* **16,** 154-160.

Vittet, D., Prandini, M. H., Berthier, R., Schweitzer, A., Martin-Sisteron, H., Uzan, G. and Dejana, E. (1996). Embryonic stem cells differentiate in vitro to endothelial cells through successive maturation steps. *Blood* **88,** 3424-3431.

Xu, C., Liguori, G., Adamson, E. D. and Persico, M. G. (1998). Cardiac differentiation is blocked in embryonic stem cells lacking Cripto-1. *Dev. Biol.* **196,** 237-247.

Zhang, J., Talbot, W. S. and Schier, A. F. (1998). Positional cloning identifies zebrafish one-eyed pinhead as a permissive EGF-related ligand required during gastrulation. *Cell* **92,** 241-251.